Eur. Phys. J. C (2021) 81:947
https://doi.org/10.1140/epjc/s10052-021-09667-8

THE EUROPEAN PHYSICAL JOURNAL C

Regular Article - Theoretical Physics

Quark and lepton flavor model with leptoquarks in a modular A_4 symmetry

Takaaki Nomura[1,a], **Hiroshi Okada**[2,3,b], **Yuta Orikasa**[4,c]

[1] College of Physics, Sichuan University, Chengdu 610065, China
[2] Asia Pacific Center for Theoretical Physics, Pohang 37673, Republic of Korea
[3] Department of Physics, Pohang University of Science and Technology, Pohang 37673, Republic of Korea
[4] Institute of Experimental and Applied Physics, Czech Technical University in Prague, 110 00 Prague 1, Czech Republic

Received: 8 July 2021 / Accepted: 16 September 2021 / Published online: 25 October 2021

Abstract We propose a quark-lepton model via leptoquarks and modular A_4 symmetry. Since the neutrino mass is induced at one-loop level mediated by down quarks as well as leptoquarks, we have to explain lepton and quark masses and mixings with a single modulus τ. Here, we find predictions for lepton and quark sectors with unified modulus τ, and show several constraints originating from leptoquarks.

1 Introduction

Since lepto-quark(LQ) bosons connect lepton and quark sectors, these models potentially explain several new physics beyond the standard model (SM); e.g., lepton(muon or electron) anomalous magnetic dipole moment $(g-2)$ [1–6], B meson decays such as $b \to s\mu\bar{\mu}$ [2,4,5,7–9] and $b \to c\ell\bar{\nu}_\ell(\ell = e, \mu, \tau)$ [4,8–10],[1] and nonzero neutrino masses [6,9,11,14]. Especially, muon $g-2$ anomaly is recently reported by E989 experiment at Fermilab combining BNL result [22], and its value is deviated from the SM by 4.2σ as follows:

$$\Delta a_\mu = (25.1 \pm 5.9) \times 10^{-10}. \tag{1.1}$$

Also, the LHCb collaboration [23] recently reported anomaly of rare B meson decays of $b \to s\mu\bar{\mu}$ that is understood as violation of lepton universality. The updated result is given by

$$\frac{BR(B^+ \to K^+\mu^-\mu^+)}{BR(B^+ \to K^+e^-e^+)} = 0.846^{+0.042+0.013}_{-0.039-0.012} \quad (1.1\,\text{GeV}^2 < q^2 < 6\,\text{GeV}^2), \tag{1.2}$$

where first(second) uncertainty is statistical(systematic) one and q^2 is the invariant mass squared for dilepton. In addition to the above phenomenologies, interestingly, the nonzero Majorana neutrino mass at one-loop can be realized without any additional symmetries by introducing appropriate LQs [12–14]. This may be natural realization of tiny neutrino mass model due to loop suppression.

Considering above issues, one finds that Yukawa flavor structure is also very important to explain them. Recently, powerful symmetries to restrict the number of parameters in Yukawa couplings, so called "modular flavor symmetries", were proposed by authors in Refs. [24,25], in which they have applied modular originated non-Abelian discrete flavor symmetries to quark and lepton sectors. One remarkable advantage of applying this symmetries is that dimensionless couplings of model can be transformed into non-trivial representations under those symmetries, and all the dimensionless values are uniquely fixed once modulus is determined in fundamental region. We then do not need the scalar fields to obtain a predictive mass matrix. Along the line of this idea, a vast reference has recently appeared in the literature, e.g., A_4 [24,26–58], S_3 [59–64], S_4 [65–76], A_5 [70,77,78], double covering of A_5 [79–81], larger groups [82], multiple modular symmetries [83], and double covering of A_4 [84,85], S_4 [86,87], and the other types of groups [88–93] in which masses, mixing, and CP phases for the quark

[1] The anomaly of $b \to c\ell\bar{\nu}_\ell$ processes are observed in experiments [15–21], and LQ model is one of the most promising explanations on this anomaly.

[a] e-mail: nomura@scu.edu.cn
[b] e-mail: hiroshi.okada@apctp.org
[c] e-mail: Yuta.Orikasa@utef.cvut.cz (corresponding author)

and/or lepton have been predicted.[2] Moreover, a systematic approach to understand the origin of CP transformations has been discussed in Ref. [102], and CP/flavor violation in models with modular symmetry was discussed in Refs. [56,103–105], and a possible correction from Kähler potential was discussed in Ref. [106]. Furthermore, systematic analysis of the fixed points (stabilizers) has been discussed in Ref. [107]. A very recent paper of Ref. [108] finds a favorable fixed point $\tau = \omega$ among three fixed points, which are the fundamental domain of PSL(2, Z), by systematically analyzing the stabilized moduli values in the possible configurations of flux compactifications as well as investigating the probabilities of moduli values. It is then interesting to discuss a LQ model under the framework of modular flavor symmetry since we are motivated to consider lepton and quark sector together as a LQ connect these sectors and some predictions in both sector can be expected.

In this paper, we focus on the quark and lepton masses and mixings based on a LQ model in Ref. [14], introducing modular A_4 symmetry to reduce free parameters of Yukawa couplings. Since the quark sector connects to the lepton sector via LQ, charge assignments for quarks(leptons) directly affect the leptons(quarks). In this sense, it would be a good motivation towards unification of quark and lepton flavor in A_4 modular symmetry.

This paper is organized as follows. In Sect. 2, we review our model of quark and lepton. In Sect. 3, we have numerical analysis and show several results for normal and inverted hierarchies. We conclude in Sect. 4. In appendix, we summarize several features of modular A_4 symmetry.

2 Model

In this section, we review our model. It is known that introducing proper leptoquarks lead us to a radiative seesaw model without any additional symmetries such as Z_2. Here, we introduce two types of leptoquarks η and Δ based on Ref. [14]. The color-triplet η has $SU(2)_L$ doublet with 1/6 hypercharge, and the color-antitriplet Δ has $SU(2)_L$ triplet with 1/3 hypercharge, where these new bosons and their charges are summarized in Table 1. Then, the valid Lagrangian to induce the quark and lepton mass matrices is given by

$$-\mathcal{L}_Y^q = y_{ij}^u \bar{u}_{R_i}(i\sigma_2)H^* Q_{L_j} + y_{ij}^d \bar{d}_{R_i} H Q_{L_j} + \text{h.c.}, \quad (2.1)$$

$$-\mathcal{L}_Y^\ell = h_{ij}\bar{e}_{R_i} H L_{L_j} + \text{h.c.}. \quad (2.2)$$

[2] For interest readers, we provide some literature reviews, which are useful to understand the non-Abelian group and its applications to flavor structure [94–101].

The Lagrangian for the mixing between the quark and lepton and nontrivial potential are given by

$$-\mathcal{L}_Y^{mix} = f_{ij}\overline{d_{R_i}}\eta^T(i\sigma_2)L_{L_j} + g_{ij}\overline{Q_{L_i}^c}(i\sigma_2)\Delta L_{L_j} + \text{h.c.}, \quad (2.3)$$

$$\mathcal{V} \supset -\mu H^\dagger \Delta\eta + \text{h.c.}, \quad (2.4)$$

where $(i, j) = 1-3$ are family indices, σ_2 is the second Pauli matrix, and H is the SM Higgs field that develops a nonzero VEV, which is symbolized by $\langle H\rangle \equiv v/\sqrt{2} \approx 246/\sqrt{2}$ GeV, and H has nonzero modular weight. Here, we parameterize components of the scalars as follows:

$$H = \begin{bmatrix} w^+ \\ \frac{v+\phi+iz}{\sqrt{2}} \end{bmatrix}, \quad \eta = \begin{bmatrix} \eta_{2/3} \\ \eta_{-1/3} \end{bmatrix}, \quad \Delta = \begin{bmatrix} \frac{\delta_{1/3}}{\sqrt{2}} & \delta_{4/3} \\ \delta_{-2/3} & -\frac{\delta_{1/3}}{\sqrt{2}} \end{bmatrix}, \quad (2.5)$$

where the subscript of the fields represents the electric charge, and w^+ and z are absorbed by the longitudinal component of the W^+ and Z bosons, respectively. Due to the μ term in Eq. (2.4), the charged components with 1/3 and 2/3 electric charges mix each other. Here, we parametrize their mixing matrices and mass eigenstates as follows:

$$\begin{bmatrix} \eta_{i/3} \\ \delta_{i/3} \end{bmatrix} = O_i \begin{bmatrix} A_i \\ B_i \end{bmatrix}, \quad O_i \equiv \begin{bmatrix} c_{a_i} & s_{a_i} \\ -s_{a_i} & c_{a_i} \end{bmatrix}, \quad (i = 1, 2), \quad (2.6)$$

where their masses are denoted as m_{A_i} and m_{B_i} respectively. The interactions in terms of the mass eigenstates can be written as

$$-\mathcal{L}_Y^q \approx m_{u_{ij}}\bar{u}_{R_i}u_{L_j} + m_{d_{ij}}\bar{d}_{R_i}d_{L_j} + \text{h.c.}, \quad (2.7)$$

$$-\mathcal{L}_Y^\ell \approx m_{\ell_{ij}}\bar{e}_{R_i}\ell_{L_j} + \text{h.c.}, \quad (2.8)$$

$$-\mathcal{L}_Y^{mix} \approx f_{ij}\overline{d_{R_i}}\nu_{L_j}(c_{a_1}A_1^* + s_{a_1}B_1^*) - \frac{g_{ij}}{\sqrt{2}}\overline{d_{L_i}^c}\nu_{L_j}(-s_{a_1}A_1 + c_{a_1}B_1) \quad (2.9)$$

$$- f_{ij}\overline{d_{R_i}}\ell_{L_j}(c_{a_2}A_2 + s_{a_2}B_2) - \frac{g_{ij}}{\sqrt{2}}\overline{u_{L_i}^c}\ell_{L_j}(-s_{a_1}A_1 + c_{a_1}B_1) \quad (2.10)$$

$$- g_{ij}\overline{d_{L_i}^c}\ell_{L_j}\delta_{4/3} + g_{ij}\overline{u_{L_i}^c}\nu_{L_j}(-s_{a_2}A_2^* + c_{a_2}B_2^*) + \text{h.c.}, \quad (2.11)$$

where we define $m_{u_{ij}} \equiv \frac{vy_{ij}^u}{\sqrt{2}}$, $m_{d_{ij}} \equiv \frac{vy_{ij}^d}{\sqrt{2}}$, and $m_{\ell_{ij}} \equiv \frac{vh_{ij}}{\sqrt{2}}$.

The next task is to determine the matrices of y^u, y^d, h, f, g via modular A_4 symmetry. In the quark sector, we assign Q_L to be **3** and -2, $\bar{u}_R$ to be $\{1, 1'', 1'\}$ and -4, and $\bar{d}_R$ to be $\{1, 1'', 1'\}$ and 0 under A_4 and $-k$, respectively. This assignment is the same as the one in Ref. [45], and it is already

Table 1 Charge assignments of the LQ bosons η and Δ under $SU(3)_C \times SU(2)_L \times U(1)_Y \times A_4$ where k_I is the number of modular weight

	η	Δ
$SU(3)_C$	**3**	$\bar{\mathbf{3}}$
$SU(2)_L$	**2**	**3**
$U(1)_Y$	$\frac{1}{6}$	$\frac{1}{3}$
A_4	**1**	**1**
$-k_I$	-2	-2

known that allowed region [30]. Thus, we will work on the same τ region of the lepton sector in our numerical analysis. The up-type quark mass matrix is written as:

$$y^u = \begin{pmatrix} a_u & 0 & 0 \\ 0 & a_c & 0 \\ 0 & 0 & a_t \end{pmatrix} \left[\begin{pmatrix} f_1 & f_3 & f_2 \\ f_2 & f_1 & f_3 \\ f_3 & f_2 & f_1 \end{pmatrix} + \begin{pmatrix} g_{u1} & 0 & 0 \\ 0 & g_{u2} & 0 \\ 0 & 0 & g_{u3} \end{pmatrix} \begin{pmatrix} f_1' & f_3' & f_2' \\ f_2' & f_1' & f_3' \\ f_3' & f_2' & f_1' \end{pmatrix} \right], \tag{2.12}$$

where $Y_3^{(6)} \equiv [f_1, f_2, f_3]^T$ and $Y_{3'}^{(6)} \equiv [f_1', f_2', f_3']^T$, $g_{u1} = \alpha_u'/\alpha_u$, $g_{u2} = \beta_u'/\beta_u$ and $g_{u3} = \gamma_u'/\gamma_u$ are complex parameters, and a_u, a_c and a_t can be used to fit the masses of up quarks. The explicit forms of f_i and f_i' are summarized in Appendix. Then m_u is diagonalized by two unitary matrices as $D_u = V_{u_R}^\dagger m_u V_{u_L}$, where $D_u \equiv \mathrm{diag}(m_u, m_c, m_t)$ is mass eigenvalues. Therefore, we find $|D_u|^2 = V_{u_L}^\dagger m_u^\dagger m_u V_{u_L}$.

On the other hand, the down-type quark mass matrix is given as:

$$y^d = \begin{pmatrix} a_d & 0 & 0 \\ 0 & a_s & 0 \\ 0 & 0 & a_b \end{pmatrix} \begin{pmatrix} y_1 & y_3 & y_2 \\ y_2 & y_1 & y_3 \\ y_3 & y_2 & y_1 \end{pmatrix}, \tag{2.13}$$

where and a_d, a_s and a_b can be used to fit the masses of down quarks, and $Y_3^{(2)} \equiv [y_1, y_2, y_3]^T$ in Appendix. Then m_d is diagonalized by two unitary matrices as $D_d = V_{d_R}^\dagger m_d V_{d_L}$, where $D_d \equiv \mathrm{diag}(m_d, m_s, m_b)$ is mass eigenvalues. Therefore, we find $|D_d|^2 = V_{d_L}^\dagger m_d^\dagger m_d V_{d_L}$. Finally, we get the observable mixing matrix V_{CKM} as follows:

$$V_{CKM} = V_{u_L}^\dagger V_{d_L}. \tag{2.14}$$

2.1 Lepton sector

Now let us move on the lepton sector. We assign L_L to be **3** and -2 and $\bar{e}_R$ to be $\{1, 1'', 1'\}$ and 0 under A_4 and $-k$, respectively. Here, both of the leptoquark scalars are assigned to be true A_4 singlets with -2 modular weight. The assignments of A_4 and $-k$ are also summarized in Tables 1 and 2. Under these assignments, we can write down the concrete matrices as follows:

$$h = \begin{bmatrix} a_\ell & 0 & 0 \\ 0 & b_\ell & 0 \\ 0 & 0 & c_\ell \end{bmatrix} \begin{bmatrix} y_1 & y_3 & y_2 \\ y_2 & y_1 & y_3 \\ y_3 & y_2 & y_1 \end{bmatrix}, \tag{2.15}$$

$$f = \begin{bmatrix} a_\eta & 0 & 0 \\ 0 & b_\eta & 0 \\ 0 & 0 & c_\eta \end{bmatrix} \begin{bmatrix} y_1' & y_3' & y_2' \\ y_2' & y_1' & y_3' \\ y_3' & y_2' & y_1' \end{bmatrix}, \tag{2.16}$$

$$\begin{aligned} g = {} & aY_1^{(6)} \begin{bmatrix} 1 & 0 & 0 \\ 0 & 0 & 1 \\ 0 & 1 & 0 \end{bmatrix} + \frac{b}{3} \begin{bmatrix} 2f_1 & -f_3 & -f_2 \\ -f_3 & 2f_2 & -f_1 \\ -f_2 & -f_1 & 2f_3 \end{bmatrix} \\ & + \frac{c}{2} \begin{bmatrix} 0 & f_3 & -f_2 \\ -f_3 & 0 & f_1 \\ f_2 & -f_1 & 0 \end{bmatrix} \\ & + \frac{b'}{3} \begin{bmatrix} 2f_1' & -f_3' & -f_2' \\ -f_3' & 2f_2' & -f_1' \\ -f_2' & -f_1' & 2f_3' \end{bmatrix} + \frac{c'}{2} \begin{bmatrix} 0 & f_3' & -f_2' \\ -f_3' & 0 & f_1' \\ f_2' & -f_1' & 0 \end{bmatrix} \end{aligned} \tag{2.17}$$

where $Y_3^{(4)} \equiv [y_1', y_2', y_3']^T$ in Appendix.

The charged-lepton sector after spontaneous symmetry breaking is given by

$$-\mathcal{L}_Y^\ell = v \frac{h_{ij}}{\sqrt{2}} \ell_{L_i} e_{R_j} + \text{h.c.}. \tag{2.18}$$

Then $m_\ell (\equiv vh/\sqrt{2})$ is diagonalized by two unitary matrices as $D_\ell = V_{\ell_R}^\dagger m_\ell V_{\ell_L}$, where $D_\ell \equiv \mathrm{diag}(m_e, m_\mu, m_\tau)$ is mass eigenvalues. Therefore, we find $|D_\ell|^2 = V_{\ell_L}^\dagger m_\ell^\dagger m_\ell V_{\ell_L}$. The active neutrino mass matrix m_ν is given at one-loop level through the following interactions:

$$\begin{aligned} -L_Y^\ell = {} & F_{aj} \overline{d'_{R_a}} \nu_{L_j} (c_{a_1} A_1 + s_{a_1} B_1) \\ & - G_{aj} \overline{d'^c_{L_a}} \nu_{L_j} (-s_{a_1} A_1 + c_{a_1} B_1), \end{aligned} \tag{2.19}$$

where $F \equiv V_{d_R}^\dagger f$ and $G \equiv V_{d_L}^T g$ and d' is mass eigenstate. Then, the neutrino masss matrix in Fig. 1 is given at one-loop level as follows:

$$\begin{aligned} (m_\nu)_{ij} = {} & s_{2a_1} \frac{3}{4(4\pi)^2} \left[1 - \frac{m_{A_1}^2}{m_{B_1}^2} \right] \\ & \times \sum_{i=1}^{3} \left[F_{ia}^T D_{d_a} G_{aj} + G_{ia}^T D_{d_a} F_{aj} \right] F_I(r_{A_1}, r_{D_{d_i}}), \end{aligned} \tag{2.20}$$

$$F_I(r_1, r_2) = \frac{r_1(r_2 - 1)\ln r_1 - r_2(r_1 - 1)\ln r_2}{(r_1 - 1)(r_2 - 1)(r_1 - r_2)}, \quad (r_1 \neq 1), \tag{2.21}$$

Table 2 Charge assignments of the SM fermions under $SU(3)_C \times SU(2)_L \times U(1)_Y \times A_4$ where k_I is the number of modular weight

	Fermions				
	Q_L	$\bar{u}_R$	d_R	L_L	$\bar{e}_R$
$SU(3)_C$	**3**	$\bar{\mathbf{3}}$	$\bar{\mathbf{3}}$	**1**	**1**
$SU(2)_L$	**2**	**1**	**1**	**2**	**1**
$U(1)_Y$	$\frac{1}{6}$	$-\frac{2}{3}$	$\frac{1}{3}$	$-\frac{1}{2}$	1
A_4	**3**	**1, 1″, 1′**	**1, 1″, 1′**	**3**	**1, 1″, 1′**
$-k_I$	-2	-4	0	-2	0

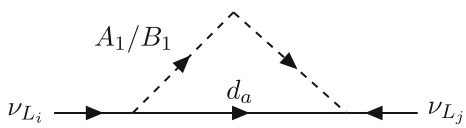

Fig. 1 One-loop diagrams for generating the neutrino mass matrix

where we define $r_{A_1} \equiv (m_{A_1}/m_{B_1})^2$ and $r_{D_{d_i}} \equiv (D_{d_i}/m_{B_1})^2$. m_ν is diagonalzied by a unitary matrix V_ν; $D_\nu \equiv V_\nu^T m_\nu V_\nu$. Here, we define a modified neutrino mass matrix as $\tilde{m}_\nu \equiv m_\nu/s_{2a_1}$. Then, we rewrite this diagonalization in terms of the modified form $\tilde{D}_\nu \equiv V_\nu^T \tilde{m}_\nu V_\nu$. Thus, we fix s_{2a_1} by

$$(\mathrm{NH}) : s_{2a_1}^2 = \frac{|\Delta m^2_{\mathrm{atm}}|}{\tilde{D}^2_{\nu_3} - \tilde{D}^2_{\nu_1}}, \quad (\mathrm{IH}) : s_{2a_1}^2 = \frac{|\Delta m^2_{\mathrm{atm}}|}{\tilde{D}^2_{\nu_2} - \tilde{D}^2_{\nu_3}}, \tag{2.22}$$

where $\tilde{m}_\nu$ is diagonalized by $V_\nu^\dagger(\tilde{m}_\nu^\dagger \tilde{m}_\nu)V_\nu = (\tilde{D}^2_{\nu_1}, \tilde{D}^2_{\nu_2}, \tilde{D}^2_{\nu_3})$ and $\Delta m^2_{\mathrm{atm}}$ is the atmospheric neutrino mass-squared difference. Here, NH and IH respectively stand for the normal hierarchy and the inverted hierarchy. Subsequently, the solar neutrino mass-squared difference is depicted in terms of s_{2a_1} as follows:

$$\Delta m^2_{\mathrm{sol}} = s^2_{2a_1}(\tilde{D}^2_{\nu_2} - \tilde{D}^2_{\nu_1}). \tag{2.23}$$

This should be within the experimental value, where we adopt NuFit 5.0 [109] to our numerical analysis later. The neutrinoless double beta decay is also given by

$$\begin{aligned}\langle m_{ee}\rangle = s_{2a_1}|&\tilde{D}_{\nu_1}\cos^2\theta_{12}\cos^2\theta_{13} \\ &+ \tilde{D}_{\nu_2}\sin^2\theta_{12}\cos^2\theta_{13}e^{i\alpha_2} \\ &+ \tilde{D}_{\nu_3}\sin^2\theta_{13}e^{i(\alpha_3-2\delta_{CP})}|,\end{aligned} \tag{2.24}$$

which may be able to observed by KamLAND-Zen in future [110]. The observed mixing matrix of lepton sector [111] is given by $V_{\mathrm{PMNS}} \equiv V_{\ell_L}^\dagger V_\nu$.

3 Numerical analysis

Here, we perform numerical analysis. Before searching for allowed region, we fix some mass parameters as $m_{A_2} = m_{A_1}$ and $m_{B_2} = m_\delta = m_{B_1}$, where we require degenerate masses for the components of η and Δ to suppress the oblique parameters ΔS and ΔT. Notice here that our theoretical parameters $a_{u,c,t}, a_{d,s,b}, a_\ell, b_\ell, c_\ell$ are used to determined the experimental masses for quarks and charged-leptons. Thus, only the following input parameters are randomly selected in the range of

$$\begin{aligned}&(m_{A_1}, m_{B_1}) \in [1\,,\,100\,]\ \mathrm{TeV}, \\ &|g_{u1,u2,u3}| \in \left[10^{-5},\ 1.5\right], \\ &(|a_\eta|, |b_\eta|, |c_\eta|, |a|, |b|, |c|, |b'|, |c'|) \in \left[10^{-5},\ 10\right].\end{aligned} \tag{3.1}$$

Above the range, we have numerical analysis in cases for quark and lepton, where experimental data in the quark sector should be within the range at 3σ. While the one in the lepton sector is discussed in the range within 3σ (yellow dots) and 5σ (red dots) applying χ^2 analysis in Nufit 5.0.

3.1 NH

For NH case, we show our results of lepton sector in Figs. 2, 3, 4, 5. In Fig. 2, allowed value of τ is shown where yellow(red) points present the values within $3(5)\sigma$. One finds that allowed space is rather localized. Especially, the region at nearby $\tau \sim 1.75i$ would be interesting since it is close to the fixed point that has a remnant Z_3 symmetry. In Fig. 3, we demonstrate allowed region of δ_{CP} in terms of $\sum m_i$. $\sum m_i$ is rather localized at $0.06-0.08$ eV while whole the region is allowed for δ_{CP}. Moreover, almost all the points are within the cosmological constraint ~ 0.12 eV [112]. In Fig. 4, we present allowed region of neutrinoless double beta decay $\langle m_{ee}\rangle$ in terms of the lightest neutrino mass m_1. $\langle m_{ee}\rangle$ is allowed up to 0.025 eV while m_1 is allowed up to 0.0025 eV. Moreover, allowed region of m_1 is localized at around 10^{-6} eV indicating tiny mass of the lightest neutrino mass. In Fig. 5, we

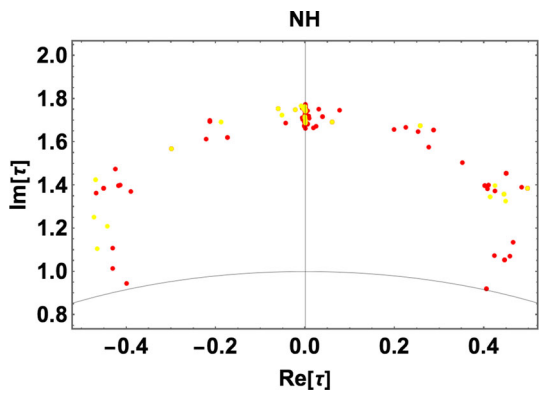

Fig. 2 Allowed value of τ. Yellow and red points present the values within 3 and 5σ

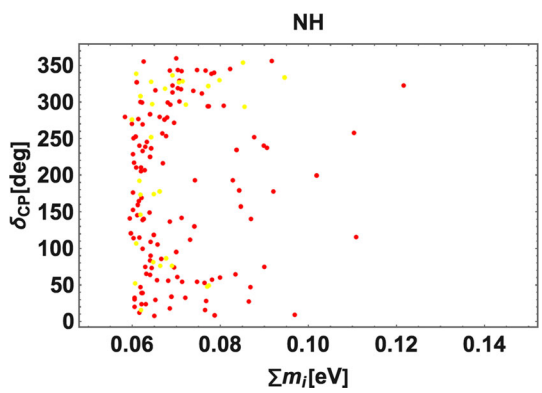

Fig. 3 Allowed region of δ_{CP} in terms of $\sum m_i$

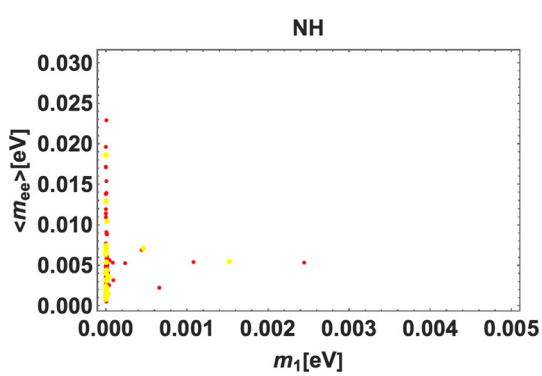

Fig. 4 Allowed region of the mass of neutrinoless double beta decay in terms of the lightest neutrino mass

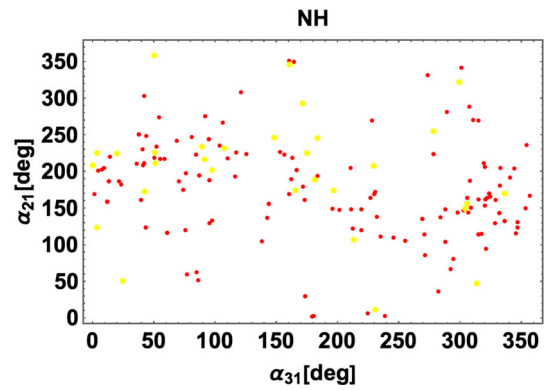

Fig. 5 Allowed region of Majorana phases α_{21} in terms of α_{31}

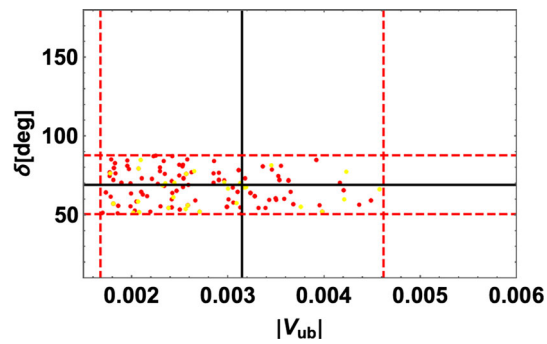

Fig. 6 The CP phase of quark δ versus (1, 3) component of CKM matrix. The red dashed lines represent 3σ experimental bounds

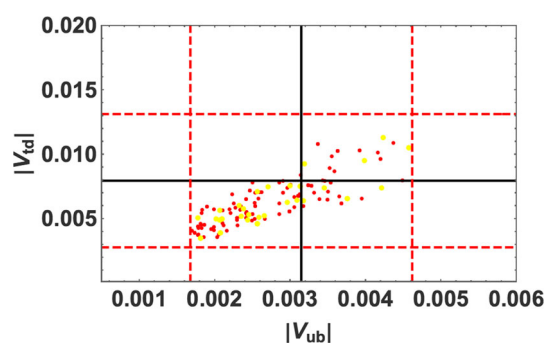

Fig. 7 $|V_{ub}|$ versus $|V_{td}|$

depict allowed region of Majorana phases α_{21} and α_{31}. Both are allowed for whole the region but there would be tendency that α_{21} is localized at around 180°.

In addition to the lepton sector, we will search for our allowed region of quark sector in Figs. 6, 7, 8. Here, the dotted red line at 3σ interval while the black line is best fit value. And the yellow(red) points correspond to $3(5)\sigma$ of the lepton sector where τ is commonly used.

In Fig. 6, we show the CP phase of quark δ in term of (1, 3) component of CKM matrix; $|V_{ub}|$, and find whole the region is allowed at 3σ interval. In Fig. 7, we show $|V_{ub}|$ and $|V_{td}|$, and found that there is a weak linearly correlation between them. In Fig. 8, we show $|V_{cb}|$ and $|V_{ub}|$, and find that there is also a weak linear correlation between them.

Bench mark point for NH: We also give a benchmark point to satisfy the quark and lepton masses and mixings as well as phases in the left sides of Tables 3 and 4 , where we extracted a value at nearby $\tau = 1.75i$. The corresponding lepton and neutrino mixings are given by

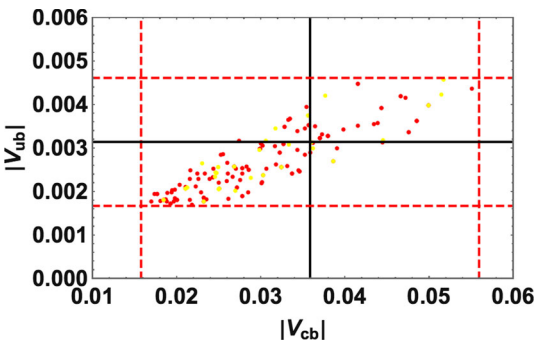

Fig. 8 $|V_{cb}|$ versus $|V_{ub}|$

$$V_{\ell_L} = \begin{bmatrix} -0.75+0.00017i & 0.35-0.000026i & -0.56 \\ 0.20-0.000012i & -0.68+0.000074i & -0.70-0.000040i \\ -0.63+0.00013i & -0.64+0.000077i & 0.44+0.000044i \end{bmatrix}, \tag{3.2}$$

$$V_\nu = \begin{bmatrix} -0.91-0.20i & 0.26-0.075i & -0.22-0.027i \\ 0.23+0.018i & -0.045-0.28i & -0.87-0.33i \\ -0.13+0.24i & -0.25+0.88i & -0.25-0.15i \end{bmatrix}. \tag{3.3}$$

And the quark mixings are given by

$$V_{u_L} = \begin{bmatrix} -0.75-0.057i & 0.41+0.24i & -0.46+0.0034i \\ -0.62+0.017i & -0.31-0.068i & 0.71-0.0045i \\ 0.19-0.071i & 0.76+0.30i & 0.53-0.0015i \end{bmatrix}, \tag{3.4}$$

$$V_{d_L} = \begin{bmatrix} -0.64+0.000077i & -0.63+0.00013i & -0.44-0.000044i \\ -0.68+0.000074i & 0.20-0.000012i & 0.70+0.000040i \\ 0.35-0.000026i & -0.75+0.00017i & 0.56 \end{bmatrix}. \tag{3.5}$$

3.2 IH

In case of IH, we obtain less allowed parameter points compared to the case of NH since it is more difficult to fit the data. Since there are no points within 3σ region but few points within 5σ region, we will explain the tendency instead of showing scattering plots. The value of τ is interestingly localized at nearby two fixed points i and $1.74i$, each of which has remnant symmetry of Z_2 and Z_3. $\sum m_i$ is localized at 0.10–0.12 eV while δ_{CP} is allowed for the range of 150°–360°. Moreover, almost all the points are within the cosmological constraint ~ 0.12 eV that is similar to the NH case. $\langle m_{ee}\rangle$ is localized at around 0.016–0.024 eV while m_1 is allowed up to 1.2×10^{-4} eV. Moreover, m_1 is also localized at around 10^{-6} eV . α_{21} is localized at around 180°,while α_{21} is allowed for the range of 100°–360°.

In addition to the lepton sector, we discuss our allowed region of quark sector. Even though the allowed points are not so many, we might say something from our analysis as follows. As for the CP phase of quark δ in term of (1, 3) component of CKM matrix; $|V_{ub}|$, we found whole the region is allowed at 3σ interval. As for $|V_{ub}|$ and $|V_{td}|$, we find that there is a weak linearly correlation between them. As for $|V_{cb}|$ and $|V_{ub}|$, we find that there is also a weak linear correlation between them.

Bench mark point for IH: We give two interesting benchmark points; $\tau \approx 1.06i,\ 1.76i$ to satisfy the quark and lepton masses and mixings as well as phases in the center and right sides of Tables 3 and 4 . The lepton and neutrino mixings are given by

$\tau \approx 1.06i$:

$$V_{\ell_L} = \begin{bmatrix} -0.65+0.0068i & 0.72+0.00024i & -0.25+0.00061i \\ -0.47+0.0067i & -0.64+0.0012i & -0.61+0.00072i \\ -0.60+0.0068i & -0.28+0.00098i & 0.75+0.000042i \end{bmatrix}, \tag{3.6}$$

$$V_\nu = \begin{bmatrix} -0.63+0.12i & 0.053-0.029i & -0.13-0.75i \\ 0.090+0.11i & 0.14+0.98i & 0.015-0.089i \\ -0.75+0.10i & 0.12+0.097i & 0.068+0.63i \end{bmatrix}, \tag{3.7}$$

$\tau \approx 1.76i$: (3.8)

$$V_{\ell_L} = \begin{bmatrix} -0.21-0.000031i & 0.80-0.0015i & 0.56+0.000052i \\ 0.63-0.00065i & -0.33+0.00026i & 0.70+0.00032i \\ 0.75-0.00091i & 0.50-0.0010i & -0.44-0.00036i \end{bmatrix}, \tag{3.9}$$

$$V_\nu = \begin{bmatrix} -0.010+0.016i & 0.063-0.098i & -0.87+0.48i \\ 0.28-0.037i & -0.77+0.56i & -0.12+0.014i \\ 0.53+0.80i & 0.25+0.13i & 0.016+0.0094i \end{bmatrix}. \tag{3.10}$$

The quark mixings are given by

$\tau \approx 1.06i$:

$$V_{u_L} = \begin{bmatrix} -0.59+0.26i & -0.18-0.067i & -0.71-0.23i \\ -0.55+0.21i & -0.50-0.030i & 0.61+0.18i \\ -0.41+0.28i & 0.84-0.062i & 0.20+0.080i \end{bmatrix}, \tag{3.11}$$

$$V_{d_L} = \begin{bmatrix} -0.60+0.0068i & -0.28+0.00096i & -0.75-0.000044i \\ -0.47+0.0067i & -0.64+0.0011i & 0.61-0.00072i \\ -0.65+0.0068i & 0.72+0.00022i & 0.25-0.00061i \end{bmatrix}, \tag{3.12}$$

$\tau \approx 1.76i$:

$$V_{u_L} = \begin{bmatrix} -0.76-0.042i & 0.43+0.199 & -0.45+0.0188i \\ -0.62+0.015i & -0.33-0.052i & 0.71-0.026i \\ 0.19-0.054i & 0.78+0.23i & 0.54-0.014i \end{bmatrix}, \tag{3.13}$$

$$V_{d_L} = \begin{bmatrix} -0.64+0.00066i & -0.63+0.0011i & -0.44-0.00039i \\ -0.68+0.00064i & 0.21-0.00013i & 0.70+0.00037i \\ 0.35-0.00023i & -0.75+0.0015i & 0.56+0.000089i \end{bmatrix}. \tag{3.14}$$

4 Conclusions

We have proposed a LQ model to explain the masses and mixings for quark and lepton, introducing modular A_4 symmetry. Due to nature of LQ model that lepton(quark) directly connects to the quark(lepton) via LQ, a single modulus number has to be applied that leads to a good motivation towards unification of quark and lepton flavor in A_4 modular symme-

Table 3 Numerical values of parameters and observables at the best fit points of NH and IH

Lepton	NH ($\tau \approx 1.75i$)	IH ($\tau \approx 1.06i$)	IH ($\tau \approx 1.76i$)
τ	$-0.0000945 + 1.75i$	$-0.000689 + 1.06i$	$-0.000829 + 1.76i$
a_η	$-0.23 - 1.4i$	$-0.31 + 0.013i$	$-4.1 + 4.3i$
b_η	$-0.38 + 1.3i$	$-0.045 - 0.027i$	$-0.0014 + 0.0032i$
c_η	$0.0077 - 0.031i$	$0.0014 - 0.000047i$	$-0.0023 + 0.0035i$
a	$0.00016 + 0.00011i$	$3.0 + 0.98i$	$0.0085 + 0.025i$
b	$-0.017 + 0.0013i$	$0.00014 + 0.00015i$	$-0.096 + 0.041i$
c	$-0.00030 - 0.00010i$	$0.0056 - 0.0021i$	$-1.8 + 4.5i$
b'	$0.00014 - 0.000016i$	$0.000024 + 0.000016i$	$-0.00011 + 0.00011i$
c'	$-0.21 - 0.27i$	$-0.15 + 0.031i$	$-0.0000034 - 0.000060i$
$[\alpha_e, \beta_e, \gamma_e]$	$[0.0002, 9.3 \times 10^{-7}, 0.003]$	$[0.0005, 10^{-5}, 0.007]$	$[9.1 \times 10^{-7}, 1.9 \times 10^{-4}, 0.003]$
$\sin^2\theta_{12}$	0.32	0.28	0.33
$\sin^2\theta_{23}$	0.56	0.46	0.58
$\sin^2\theta_{13}$	0.024	0.024	0.022
δ^ℓ_{CP}	328°	170°	335°
$[\alpha_{21}, \alpha_{31}]$	[169°, 336°]	[167°, 159°]	[157°, 130°]
$\sum m_i$	0.071 eV	0.11 eV	0.11 eV
s_{2a_1}	4.6×10^{-9}	5.7×10^{-5}	1.9×10^{-9}
$\langle m_{ee} \rangle$	3.2 meV	21 meV	19 meV
$[m_{A_1}, m_{B_1}]$	[18, 6.0] TeV	[37, 37] TeV	[33, 39] TeV
$\sqrt{\chi^2}$	2.9	4.8	4.5

Table 4 Numerical values of parameters and observables at the best fit points of NH and IH

Quark	NH ($\tau \approx 1.75i$)	IH ($\tau \approx 1.06i$)	IH ($\tau \approx 1.76i$)
τ	$-0.0000945 + 1.75i$	$-0.000689 + 1.06i$	$-0.000829 + 1.76i$
a_u	1.3×10^{-7}	8.2×10^{-8}	1.1×10^{-5}
a_c	4.6×10^{-5}	4.2×10^{-5}	0.0007
a_t	0.017	0.017	0.22
g_{u1}	$0.00066 + 0.0016i$	$-0.00013 + 0.013i$	$0.57 - 0.35i$
g_{u2}	$0.053 + 0.30i$	$0.094 + 0.24i$	$-0.060 - 0.41i$
g_{u3}	$0.11 + 0.0061i$	$0.091 + 0.018i$	$0.046 + 0.021i$
a_d	0.00018	0.00014	0.00047
a_s	1.2×10^{-5}	8.7×10^{-6}	5.2×10^{-5}
a_b	0.011	0.011	0.025
$\lvert V_{us}\rvert$	0.23	0.22	0.22
$\lvert V_{cb}\rvert$	0.033	0.027	0.042
$\lvert V_{ub}\rvert$	0.0031	0.0020	0.0039
δ_{CP}	58°	51°	83°

try. After giving an assignment for quark sector to reproduce the experimental results at 3σ interval, we have also constructed the lepton sector, where the neutrino mass matrix is induced at one-loop level running down quark sector, unified value of τ is used for quark and lepton.

Then, we have performed numerical analysis to search for allowed region satisfying experimental measurements for both quark and lepton sector, depending on NH and IH. In case of NH, we have found rather wide allowed space within 3σ interval and obtained tendency of observables for quark and lepton. Especially, we have found allowed region at nearby $\tau = 1.75i$ that is close to the fixed point of $\tau = i\infty$. Thus, we have also shown a promising bench mark point at around the solution.

In case of IH, we would not found the allowed region within 3σ interval, but found within 5σ interval. Although

the number of allowed point is few, we have found all the allowed regions are localized at nearby $\tau = i,\ 1.76i$, both of which are nearby fixed points. We have shown them as benchmark points. These would be tested near future.

Before closing it is worthwhile mentioning on flavor physics and collider phenomenology of our model. On hadron collider experiments such as the LHC, lepto-quarks can be pair produced via strong interactions and lower limits of their masses are given as $\mathcal{O}(1)$ TeV depending on its decay modes [113–115]. In addition the most striking signature would arise from the lepton flavor violating process at the LHC via lepto-quarks in the t-channel, $q\bar{q} \to \ell'^{+}\ell^{-}$, with final states such as $e^{\pm}\mu^{\mp}, e^{\pm}\tau^{\mp}, \mu^{\pm}\tau^{\mp}$. Taking $g = f \approx 0.1$ and 1 TeV lepto-quark mass, we find 6 event rate for $d\bar{d} \to e^{\pm}\tau^{\mp}$, which is maximum, at the 13 TeV LHC with 300 fb^{-1} luminosity; more discussion can be found in ref. [14]. For flavor physics, whenever considering radiative seesaw models, we have to consider lepton flavor violations, especially, $\mu \to e\gamma$. This gives the most stringent constraint on Yukawa couplings and masses of mediated particles which are lepto-quarks in our case. For our model, Yukawa couplings f, g can be order 1, since the lepto-quark masses has to be larger than 1 TeV from the collider analysis at LHC. Thus, our parameters are totally safe from this constraint including other $\tau \to e(\mu)\gamma$ modes. Moreover from interactions associated with the Yukawa coupling g, we may find an interesting effects on $b \to s\mu\bar{\mu}$ anomaly, which can be characterized by Wilson coefficients $C_9 = -C_{10}$ of six dimensional effective Hamiltonian $[(\bar{s}\gamma_\mu P_L b)(\bar{\mu}\gamma^\mu\mu) - (\bar{s}\gamma_\mu P_L b)(\bar{\gamma}^\mu\gamma_5\mu)]$. Experimental results tell us $\Delta C_9 \approx -1$ as new physics contribution. To get this order, we need $g \sim 0.1$, supposing 1 TeV of lepto-quark mass. However since ΔC_{10} also contributes to the process of $b \to \mu\bar{\mu}$ that gives a constraint of $\Delta C_{10} \approx 0.1$. Thus, we would need to modify the model if one wants to get the sizable anomaly of $b \to s\mu\bar{\mu}$. Yukawa coupling g (as well as f) also receives constraints from neutral meson mixings such as K-short and K-long at one-loop box diagram. Typically, $g(f)$ should be less than ~ 0.1 at 1 TeV of lepto-quark mass. We have a source of muon $g-2$ from both the Yukawa couplings g and f at one-loop level. However, assuming $g = f \approx 0.1$ and 1 TeV lepto-quark mass, the value of muon $g-2$ is at most 10^{-12} in our model that is far from the current experimental value 10^{-9}. Thus, we need to improve this model such that it does not include chiral suppression. In conclusion, we need extension of the model to resolve flavor anomalies such as muon $g-2$ and $b \to s\mu\bar{\mu}$.

Acknowledgements This research was supported by an appointment to the JRG Program at the APCTP through the Science and Technology Promotion Fund and Lottery Fund of the Korean Government. This was also supported by the Korean Local Governments–Gyeongsangbuk-do Province and Pohang City (H.O.), European Regional Development Fund-Project Engineering Applications of Microworld Physics (Grant No. CZ.02.1.01/0.0/0.0/16_019/0000766) (Y.O.). H. O. is sincerely grateful for the KIAS member.

Data Availability Statement This manuscript has no associated data or the data will not be deposited. [Authors' comment: Since our work is theoretical analysis we do not have specific data to provide.]

Appendix

The modular forms of weight 2, $Y_{\mathbf{3}}^{(2)} = [y_1, y_2, y_3]^T$, transforming as a triplet of A_4 is written in terms of Dedekind eta-function $\eta(\tau)$ and its derivative:

$$\begin{aligned}
y_1(\tau) &= \frac{i}{2\pi}\left(\frac{\eta'(\tau/3)}{\eta(\tau/3)} + \frac{\eta'((\tau+1)/3)}{\eta((\tau+1)/3)} + \frac{\eta'((\tau+2)/3)}{\eta((\tau+2)/3)} - \frac{27\eta'(3\tau)}{\eta(3\tau)}\right),\\
y_2(\tau) &= \frac{-i}{\pi}\left(\frac{\eta'(\tau/3)}{\eta(\tau/3)} + \omega^2\frac{\eta'((\tau+1)/3)}{\eta((\tau+1)/3)} + \omega\frac{\eta'((\tau+2)/3)}{\eta((\tau+2)/3)}\right),\\
y_3(\tau) &= \frac{-i}{\pi}\left(\frac{\eta'(\tau/3)}{\eta(\tau/3)} + \omega\frac{\eta'((\tau+1)/3)}{\eta((\tau+1)/3)} + \omega^2\frac{\eta'((\tau+2)/3)}{\eta((\tau+2)/3)}\right),\\
\eta(\tau) &= q^{1/24}\Pi_{n=1}^{\infty}(1-q^n), \quad q = e^{2\pi i\tau}, \quad \omega = e^{2\pi i/3}
\end{aligned} \tag{4.1}$$

Then, any multiplets of higher weight are constructed by multiplication rules of A_4, and one finds the following :

$$\begin{aligned}
&Y_{\mathbf{1}}^{(4)} = y_1^2 + 2y_2y_3, \quad Y_{\mathbf{3}}^{(4)} \equiv \begin{bmatrix} y_1' \\ y_2' \\ y_3' \end{bmatrix} = \begin{bmatrix} y_1^2 - y_2y_3 \\ y_3^2 - y_1y_2 \\ y_2^2 - y_1y_3 \end{bmatrix},\\
&Y_{\mathbf{1}}^{(6)} = y_1^2 + y_2^2 + y_3^2 - 3y_1y_2y_3,
\end{aligned} \tag{4.2}$$

$$\begin{aligned}
&Y_{\mathbf{3}}^{(6)} \equiv \begin{bmatrix} f_1 \\ f_2 \\ f_3 \end{bmatrix} = \begin{bmatrix} y_1^3 + 2y_1y_2y_3 \\ y_1^2y_2 + 2y_2^2y_3 \\ y_1^2y_3 + 2y_3^2y_2 \end{bmatrix},\\
&Y_{\mathbf{3}'}^{(6)} \equiv \begin{bmatrix} f_1' \\ f_2' \\ f_3' \end{bmatrix} = \begin{bmatrix} y_3^3 + 2y_1y_2y_3 \\ y_3^2y_1 + 2y_1^2y_2 \\ y_3^2y_2 + 2y_2^2y_1 \end{bmatrix}.
\end{aligned} \tag{4.3}$$

References

1. M. Bauer, M. Neubert, Phys. Rev. Lett. **116**(14), 141802 (2016). https://doi.org/10.1103/PhysRevLett.116.141802. arXiv:1511.01900 [hep-ph]
2. C.H. Chen, T. Nomura, H. Okada, Phys. Rev. D **94**(11), 115005 (2016). https://doi.org/10.1103/PhysRevD.94.115005. arXiv:1607.04857 [hep-ph]
3. E. Coluccio Leskow, G. D'Ambrosio, A. Crivellin, D. Müller, Phys. Rev. D **95**(5), 055018 (2017). https://doi.org/10.1103/PhysRevD.95.055018. arXiv:1612.06858 [hep-ph]
4. C.H. Chen, T. Nomura, H. Okada, Phys. Lett. B **774**, 456–464 (2017). https://doi.org/10.1016/j.physletb.2017.10.005. arXiv:1703.03251 [hep-ph]
5. T. Nomura, H. Okada, arXiv:2104.03248 [hep-ph]
6. D. Zhang, arXiv:2105.08670 [hep-ph]
7. S. Sahoo, R. Mohanta, Phys. Rev. D **91**(9), 094019 (2015). https://doi.org/10.1103/PhysRevD.91.094019. arXiv:1501.05193 [hep-ph]
8. D. Becirevic, S. Fajfer, N. Kosnik, O. Sumensari, Phys. Rev. D **94**(11), 115021 (2016). https://doi.org/10.1103/PhysRevD.94.115021. arXiv:1608.08501 [hep-ph]
9. Y. Cai, J. Gargalionis, M.A. Schmidt, R.R. Volkas, JHEP **10**, 047 (2017). https://doi.org/10.1007/JHEP10(2017)047. arXiv:1704.05849 [hep-ph]
10. Y. Sakaki, M. Tanaka, A. Tayduganov, R. Watanabe, Phys. Rev. D **88**(9), 094012 (2013). https://doi.org/10.1103/PhysRevD.88.094012. arXiv:1309.0301 [hep-ph]
11. D. Aristizabal Sierra, M. Hirsch, S.G. Kovalenko, Phys. Rev. D **77**, 055011 (2008). https://doi.org/10.1103/PhysRevD.77.055011. arXiv:0710.5699 [hep-ph]
12. I. de Medeiros Varzielas, G. Hiller, JHEP **06**, 072 (2015). https://doi.org/10.1007/JHEP06(2015)072. arXiv:1503.01084 [hep-ph]
13. G. Hiller, D. Loose, K. Schönwald, JHEP **12**, 027 (2016). https://doi.org/10.1007/JHEP12(2016)027. arXiv:1609.08895 [hep-ph]
14. K. Cheung, T. Nomura, H. Okada, Phys. Rev. D **94**(11), 115024 (2016). https://doi.org/10.1103/PhysRevD.94.115024. arXiv:1610.02322 [hep-ph]
15. M. Huschle et al. [Belle Collaboration], Phys. Rev. D **92**(7), 072014 (2015) https://doi.org/10.1103/PhysRevD.92.072014. arXiv:1507.03233 [hep-ex]
16. J.P. Lees et al. [BaBar Collaboration], Phys. Rev. Lett. **109**, 101802 (2012). https://doi.org/10.1103/PhysRevLett.109.101802. arXiv:1205.5442 [hep-ex]
17. J.P. Lees et al. [BaBar Collaboration], Phys. Rev. D **88**(7), 072012 (2013). https://doi.org/10.1103/PhysRevD.88.072012. arXiv:1303.0571 [hep-ex]
18. A. Abdesselam et al. [Belle Collaboration], arXiv:1603.06711 [hep-ex]
19. S. Hirose et al. [Belle], Phys. Rev. Lett. **118**(21), 211801 (2017). https://doi.org/10.1103/PhysRevLett.118.211801. arXiv:1612.00529 [hep-ex]
20. R. Aaij *et al.* [LHCb Collaboration], Phys. Rev. Lett. **115**, no. 11, 111803 (2015) Addendum: [Phys. Rev. Lett. **115**, no. 15, 159901 (2015)] 10.1103/PhysRevLett.115.159901, 10.1103/PhysRevLett.115.111803 [arXiv:1506.08614 [hep-ex]]
21. R. Aaij et al. [LHCb], Phys. Rev. D **97**(7), 072013 (2018). https://doi.org/10.1103/PhysRevD.97.072013. arXiv:1711.02505 [hep-ex]
22. B. Abi et al. [Muon g-2], Phys. Rev. Lett. **126**(14), 141801 (2021). https://doi.org/10.1103/PhysRevLett.126.141801. arXiv:2104.03281 [hep-ex]
23. R. Aaij et al. [LHCb], arXiv:2103.11769 [hep-ex]
24. F. Feruglio, https://doi.org/10.1142/9789813238053_0012. arXiv:1706.08749 [hep-ph]
25. R. de Adelhart Toorop, F. Feruglio, C. Hagedorn, Nucl. Phys. B **858**, 437–467 (2012). https://doi.org/10.1016/j.nuclphysb.2012.01.017. arXiv:1112.1340 [hep-ph]
26. J.C. Criado, F. Feruglio, SciPost Phys. **5**(5), 042 (2018). https://doi.org/10.21468/SciPostPhys.5.5.042. arXiv:1807.01125 [hep-ph]
27. T. Kobayashi, N. Omoto, Y. Shimizu, K. Takagi, M. Tanimoto, T.H. Tatsuishi, JHEP **11**, 196 (2018). https://doi.org/10.1007/JHEP11(2018)196. arXiv:1808.03012 [hep-ph]
28. H. Okada, M. Tanimoto, Phys. Lett. B **791**, 54–61 (2019). https://doi.org/10.1016/j.physletb.2019.02.028. arXiv:1812.09677 [hep-ph]
29. T. Nomura, H. Okada, Phys. Lett. B **797**, 134799 (2019). https://doi.org/10.1016/j.physletb.2019.134799. arXiv:1904.03937 [hep-ph]
30. H. Okada, M. Tanimoto, Eur. Phys. J. C **81**(1), 52 (2021). https://doi.org/10.1140/epjc/s10052-021-08845-y. arXiv:1905.13421 [hep-ph]
31. F.J. de Anda, S.F. King, E. Perdomo, Phys. Rev. D **101**(1), 015028 (2020). https://doi.org/10.1103/PhysRevD.101.015028. arXiv:1812.05620 [hep-ph]
32. P.P. Novichkov, S.T. Petcov, M. Tanimoto, Phys. Lett. B **793**, 247–258 (2019). https://doi.org/10.1016/j.physletb.2019.04.043. arXiv:1812.11289 [hep-ph]
33. T. Nomura, H. Okada, Nucl. Phys. B **966**, 115372 (2021). https://doi.org/10.1016/j.nuclphysb.2021.115372. arXiv:1906.03927 [hep-ph]
34. H. Okada, Y. Orikasa, arXiv:1907.13520 [hep-ph]
35. G.J. Ding, S.F. King, X.G. Liu, JHEP **09**, 074 (2019). https://doi.org/10.1007/JHEP09(2019)074. arXiv:1907.11714 [hep-ph]
36. T. Nomura, H. Okada, O. Popov, Phys. Lett. B **803**, 135294 (2020). https://doi.org/10.1016/j.physletb.2020.135294. arXiv:1908.07457 [hep-ph]
37. T. Kobayashi, Y. Shimizu, K. Takagi, M. Tanimoto, T.H. Tatsuishi, Phys. Rev. D **100**(11), 115045 (2019). [Erratum: Phys. Rev. D **101**(3), 039904 (2020)]. https://doi.org/10.1103/PhysRevD.100.115045. arXiv:1909.05139 [hep-ph]
38. T. Asaka, Y. Heo, T.H. Tatsuishi, T. Yoshida, JHEP **01**, 144 (2020). https://doi.org/10.1007/JHEP01(2020)144. arXiv:1909.06520 [hep-ph]
39. D. Zhang, Nucl. Phys. B **952**, 114935 (2020). https://doi.org/10.1016/j.nuclphysb.2020.114935. arXiv:1910.07869 [hep-ph]
40. G.J. Ding, S.F. King, X.G. Liu, J.N. Lu, JHEP **12**, 030 (2019). https://doi.org/10.1007/JHEP12(2019)030. arXiv:1910.03460 [hep-ph]
41. T. Kobayashi, T. Nomura, T. Shimomura, Phys. Rev. D **102**(3), 035019 (2020). https://doi.org/10.1103/PhysRevD.102.035019. arXiv:1912.00637 [hep-ph]
42. T. Nomura, H. Okada, S. Patra, Nucl. Phys. B **967**, 115395 (2021). https://doi.org/10.1016/j.nuclphysb.2021.115395. arXiv:1912.00379 [hep-ph]
43. X. Wang, Nucl. Phys. B **957**, 115105 (2020). https://doi.org/10.1016/j.nuclphysb.2020.115105. arXiv:1912.13284 [hep-ph]
44. H. Okada, Y. Shoji, Nucl. Phys. B **961**, 115216 (2020). https://doi.org/10.1016/j.nuclphysb.2020.115216. arXiv:2003.13219 [hep-ph]
45. H. Okada, M. Tanimoto, arXiv:2005.00775 [hep-ph]
46. M.K. Behera, S. Singirala, S. Mishra, R. Mohanta, arXiv:2009.01806 [hep-ph]
47. M.K. Behera, S. Mishra, S. Singirala, R. Mohanta, arXiv:2007.00545 [hep-ph]
48. T. Nomura, H. Okada, arXiv:2007.04801 [hep-ph]
49. T. Nomura, H. Okada, arXiv:2007.15459 [hep-ph]
50. T. Asaka, Y. Heo, T. Yoshida, Phys. Lett. B **811**, 135956 (2020). https://doi.org/10.1016/j.physletb.2020.135956. arXiv:2009.12120 [hep-ph]

51. H. Okada, M. Tanimoto, Phys. Rev. D **103**(1), 015005 (2021). https://doi.org/10.1103/PhysRevD.103.015005. arXiv:2009.14242 [hep-ph]
52. K.I. Nagao, H. Okada, arXiv:2010.03348 [hep-ph]
53. H. Okada, M. Tanimoto, JHEP **03**, 010 (2021). https://doi.org/10.1007/JHEP03(2021)010. arXiv:2012.01688 [hep-ph]
54. C.Y. Yao, J.N. Lu, G.J. Ding, JHEP **05**, 102 (2021). https://doi.org/10.1007/JHEP05(2021)102. arXiv:2012.13390 [hep-ph]
55. P. Chen, G.J. Ding, S.F. King, JHEP **04**, 239 (2021). https://doi.org/10.1007/JHEP04(2021)239. arXiv:2101.12724 [hep-ph]
56. T. Kobayashi, T. Shimomura, M. Tanimoto, arXiv:2102.10425 [hep-ph]
57. M. Kashav, S. Verma, arXiv:2103.07207 [hep-ph]
58. H. Okada, Y. Shimizu, M. Tanimoto, T. Yoshida, arXiv:2105.14292 [hep-ph]
59. T. Kobayashi, K. Tanaka, T.H. Tatsuishi, Phys. Rev. D **98**(1), 016004 (2018). https://doi.org/10.1103/PhysRevD.98.016004. arXiv:1803.10391 [hep-ph]
60. T. Kobayashi, Y. Shimizu, K. Takagi, M. Tanimoto, T.H. Tatsuishi, H. Uchida, Phys. Lett. B **794**, 114–121 (2019). https://doi.org/10.1016/j.physletb.2019.05.034. arXiv:1812.11072 [hep-ph]
61. T. Kobayashi, Y. Shimizu, K. Takagi, M. Tanimoto, T.H. Tatsuishi, PTEP **2020**(5), 053B05 (2020). https://doi.org/10.1093/ptep/ptaa055. arXiv:1906.10341 [hep-ph]
62. H. Okada, Y. Orikasa, Phys. Rev. D **100**(11), 115037 (2019). https://doi.org/10.1103/PhysRevD.100.115037. arXiv:1907.04716 [hep-ph]
63. S. Mishra, arXiv:2008.02095 [hep-ph]
64. X. Du, F. Wang, JHEP **02**, 221 (2021). https://doi.org/10.1007/JHEP02(2021)221. arXiv:2012.01397 [hep-ph]
65. J.T. Penedo, S.T. Petcov, Nucl. Phys. B **939**, 292–307 (2019). https://doi.org/10.1016/j.nuclphysb.2018.12.016. arXiv:1806.11040 [hep-ph]
66. P.P. Novichkov, J.T. Penedo, S.T. Petcov, A.V. Titov, JHEP **04**, 005 (2019). https://doi.org/10.1007/JHEP04(2019)005. arXiv:1811.04933 [hep-ph]
67. T. Kobayashi, Y. Shimizu, K. Takagi, M. Tanimoto, T.H. Tatsuishi, JHEP **02**, 097 (2020). https://doi.org/10.1007/JHEP02(2020)097. arXiv:1907.09141 [hep-ph]
68. S.F. King, Y.L. Zhou, Phys. Rev. D **101**(1), 015001 (2020). https://doi.org/10.1103/PhysRevD.101.015001. arXiv:1908.02770 [hep-ph]
69. H. Okada, Y. Orikasa, arXiv:1908.08409 [hep-ph]
70. J.C. Criado, F. Feruglio, S.J.D. King, JHEP **02**, 001 (2020). https://doi.org/10.1007/JHEP02(2020)001. arXiv:1908.11867 [hep-ph]
71. X. Wang, S. Zhou, JHEP **05**, 017 (2020). https://doi.org/10.1007/JHEP05(2020)017. arXiv:1910.09473 [hep-ph]
72. Y. Zhao, H.H. Zhang, JHEP **03**, 002 (2021). https://doi.org/10.1007/JHEP03(2021)002. arXiv:2101.02266 [hep-ph]
73. S.F. King, Y.L. Zhou, JHEP **04**, 291 (2021). https://doi.org/10.1007/JHEP04(2021)291. arXiv:2103.02633 [hep-ph]
74. G.J. Ding, S.F. King, C.Y. Yao, arXiv:2103.16311 [hep-ph]
75. X. Zhang, S. Zhou, arXiv:2106.03433 [hep-ph]
76. B.-Y. Qu, X.-G. Liu, P.-T. Chen, G.-J. Ding, arXiv:2106.11659 [hep-ph]
77. P.P. Novichkov, J.T. Penedo, S.T. Petcov, A.V. Titov, JHEP **04**, 174 (2019). https://doi.org/10.1007/JHEP04(2019)174. arXiv:1812.02158 [hep-ph]
78. G.J. Ding, S.F. King, X.G. Liu, Phys. Rev. D **100**(11), 115005 (2019). https://doi.org/10.1103/PhysRevD.100.115005. arXiv:1903.12588 [hep-ph]
79. X. Wang, B. Yu, S. Zhou, Phys. Rev. D **103**(7), 076005 (2021). https://doi.org/10.1103/PhysRevD.103.076005. arXiv:2010.10159 [hep-ph]
80. C.Y. Yao, X.G. Liu, G.J. Ding, Phys. Rev. D **103**(9), 095013 (2021). https://doi.org/10.1103/PhysRevD.103.095013. arXiv:2011.03501 [hep-ph]
81. X. Wang, S. Zhou, arXiv:2102.04358 [hep-ph]
82. A. Baur, H.P. Nilles, A. Trautner, P.K.S. Vaudrevange, Phys. Lett. B **795**, 7–14 (2019). https://doi.org/10.1016/j.physletb.2019.03.066. arXiv:1901.03251 [hep-th]
83. I. de Medeiros Varzielas, S.F. King, Y.L. Zhou, Phys. Rev. D **101**(5), 055033 (2020). https://doi.org/10.1103/PhysRevD.101.055033. arXiv:1906.02208 [hep-ph]
84. X.G. Liu, G.J. Ding, JHEP **08**, 134 (2019). https://doi.org/10.1007/JHEP08(2019)134. arXiv:1907.01488 [hep-ph]
85. P. Chen, G.J. Ding, J.N. Lu, J.W.F. Valle, Phys. Rev. D **102**(9), 095014 (2020). https://doi.org/10.1103/PhysRevD.102.095014. arXiv:2003.02734 [hep-ph]
86. P.P. Novichkov, J.T. Penedo, S.T. Petcov, Nucl. Phys. B **963**, 115301 (2021). https://doi.org/10.1016/j.nuclphysb.2020.115301. arXiv:2006.03058 [hep-ph]
87. X.G. Liu, C.Y. Yao, G.J. Ding, Phys. Rev. D **103**(5), 056013 (2021). https://doi.org/10.1103/PhysRevD.103.056013. arXiv:2006.10722 [hep-ph]
88. S. Kikuchi, T. Kobayashi, H. Otsuka, S. Takada, H. Uchida, JHEP **11**, 101 (2020). https://doi.org/10.1007/JHEP11(2020)101. arXiv:2007.06188 [hep-th]
89. Y. Almumin, M.C. Chen, V. Knapp-Pérez, S. Ramos-Sánchez, M. Ratz, S. Shukla, JHEP **05**, 078 (2021). https://doi.org/10.1007/JHEP05(2021)078. arXiv:2102.11286 [hep-th]
90. G.J. Ding, F. Feruglio, X.G. Liu, SciPost Phys. **10**, 133 (2021). https://doi.org/10.21468/SciPostPhys.10.6.133. arXiv:2102.06716 [hep-ph]
91. F. Feruglio, V. Gherardi, A. Romanino, A. Titov, JHEP **05**, 242 (2021). https://doi.org/10.1007/JHEP05(2021)242. arXiv:2101.08718 [hep-ph]
92. S. Kikuchi, T. Kobayashi, H. Uchida, arXiv:2101.00826 [hep-th]
93. P.P. Novichkov, J.T. Penedo, S.T. Petcov, JHEP **04**, 206 (2021). https://doi.org/10.1007/JHEP04(2021)206. arXiv:2102.07488 [hep-ph]
94. G. Altarelli, F. Feruglio, Rev. Mod. Phys. **82**, 2701–2729 (2010). https://doi.org/10.1103/RevModPhys.82.2701. arXiv:1002.0211 [hep-ph]
95. H. Ishimori, T. Kobayashi, H. Ohki, Y. Shimizu, H. Okada, M. Tanimoto, Prog. Theor. Phys. Suppl. **183**, 1–163 (2010). https://doi.org/10.1143/PTPS.183.1. arXiv:1003.3552 [hep-th]
96. H. Ishimori, T. Kobayashi, H. Ohki, H. Okada, Y. Shimizu, M. Tanimoto, Lect. Notes Phys. **858**, 1–227 (2012). https://doi.org/10.1007/978-3-642-30805-5
97. D. Hernandez, A.Y. Smirnov, Phys. Rev. D **86**, 053014 (2012). https://doi.org/10.1103/PhysRevD.86.053014. arXiv:1204.0445 [hep-ph]
98. S.F. King, C. Luhn, Rep. Prog. Phys. **76**, 056201 (2013). https://doi.org/10.1088/0034-4885/76/5/056201. arXiv:1301.1340 [hep-ph]
99. S.F. King, A. Merle, S. Morisi, Y. Shimizu, M. Tanimoto, New J. Phys. **16**, 045018 (2014). https://doi.org/10.1088/1367-2630/16/4/045018. arXiv:1402.4271 [hep-ph]
100. S.F. King, Prog. Part. Nucl. Phys. **94**, 217–256 (2017). https://doi.org/10.1016/j.ppnp.2017.01.003. arXiv:1701.04413 [hep-ph]
101. S.T. Petcov, Eur. Phys. J. C **78**(9), 709 (2018). https://doi.org/10.1140/epjc/s10052-018-6158-5. arXiv:1711.10806 [hep-ph]
102. A. Baur, H.P. Nilles, A. Trautner, P.K.S. Vaudrevange, Nucl. Phys. B **947**, 114737 (2019). https://doi.org/10.1016/j.nuclphysb.2019.114737. arXiv:1908.00805 [hep-th]
103. T. Kobayashi, Y. Shimizu, K. Takagi, M. Tanimoto, T.H. Tatsuishi, H. Uchida, Phys. Rev. D **101**(5) (2020). https://doi.org/10.1103/PhysRevD.101.055046. arXiv:1910.11553 [hep-ph]

104. P.P. Novichkov, J.T. Penedo, S.T. Petcov, A.V. Titov, JHEP **07**, 165 (2019). https://doi.org/10.1007/JHEP07(2019)165. arXiv:1905.11970 [hep-ph]
105. M. Tanimoto, K. Yamamoto, arXiv:2106.10919 [hep-ph]
106. M.C. Chen, S. Ramos-Sánchez, M. Ratz, Phys. Lett. B **801**, 135153 (2020). https://doi.org/10.1016/j.physletb.2019.135153. arXiv:1909.06910 [hep-ph]
107. I. de Medeiros Varzielas, M. Levy, Y.L. Zhou, JHEP **11**, 085 (2020). https://doi.org/10.1007/JHEP11(2020)085. arXiv:2008.05329 [hep-ph]
108. K. Ishiguro, T. Kobayashi, H. Otsuka, JHEP **03**, 161 (2021). https://doi.org/10.1007/JHEP03(2021)161. arXiv:2011.09154 [hep-ph]
109. I. Esteban, M.C. Gonzalez-Garcia, M. Maltoni, T. Schwetz, A. Zhou, JHEP **09**, 178 (2020). https://doi.org/10.1007/JHEP09(2020)178. arXiv:2007.14792 [hep-ph]
110. A. Gando et al. [KamLAND-Zen], Phys. Rev. Lett. **117**(8), 082503 (2016). https://doi.org/10.1103/PhysRevLett.117.082503. arXiv:1605.02889 [hep-ex]
111. Z. Maki, M. Nakagawa, S. Sakata, Prog. Theor. Phys. **28**, 870–880 (1962). https://doi.org/10.1143/PTP.28.870
112. P.A. Zyla et al. (Particle Data Group), Prog. Theor. Exp. Phys. **2020**, 083C01 (2020)
113. G. Aad et al. [ATLAS], Eur. Phys. J. C **81**(4), 313 (2021). https://doi.org/10.1140/epjc/s10052-021-09009-8. arXiv:2010.02098 [hep-ex]
114. G. Aad et al. [ATLAS], JHEP **06**, 179 (2021). arXiv:2101.11582 [hep-ex]
115. A.M. Sirunyan et al. [CMS], Phys. Lett. B **819**, 136446 (2021). arXiv:2012.04178 [hep-ex]